CAMERA AUTOCALIBRATION AND HOROPTER CURVES

JOSÉ IGNACIO RONDA*, ANTONIO VALDÉS**, AND FERNANDO JAUREGUIZAR*

* Grupo de Tratamiento de Imágenes	** Dep. de Geometría y Topología
Universidad Politécnica de Madrid	Universidad Complutense de Madrid
E-28040 Madrid, Spain	E-28040 Madrid, Spain
{jir,fjn}@gti.ssr.upm.es	Antonio_Valdes@mat.ucm.es

ABSTRACT. We describe a new algorithm for the obtainment of the affine and Euclidean calibration of a camera under general motion. The algorithm exploit the relationships of the horopter curves associated to each pair of cameras with the plane at infinity and the absolute conic. Using these properties we define cost functions whose minimization by means of general purpose techniques provides the required calibration. The experiments show the good convergence properties, computational efficiency and robust performance of the new techniques.

Keywords: camera autocalibration, horopter, projective geometry, nonlinear optimization.

1. INTRODUCTION

The seminal paper [2] was the first to show the possibility of calibrating a camera from a set of views, avoiding the use of any kind of calibrating object. Their method was based in the so-called Kruppa equations, which permit to locate the plane at infinity and the absolute conic in it, so recovering the Euclidean structure of space.

Additional objects and concepts came later to provide alternative tools and methods to solve the self-calibration problem. In [18] the absolute quadric was introduced. This is a singular imaginary quadric in the dual space $\mathbf{P}^{3\star}$ which encodes simultaneously the position of the plane at infinity and the absolute conic. In [12] the homographies between images induced by the plane at infinity are employed to obtain the unimodular constraint from which the plane at infinity can be found. The key observation of this work is that for the plane at infinity the associated homography is conjugated to a rotation and therefore its eigenvalues are all of them of equal modulus. Other approaches to self-calibration can be found in [4] and [7].

Another natural geometric object associated to a pair of identically calibrated cameras is the horopter curve, defined as the set of points in space which have the same image coordinates in both cameras, and generically is a twisted cubic. They were introduced in modern computer vision by Maybank in [9], appearing as one of the irreducible components of the quartic curve obtained as intersection of two ambiguous surfaces. Some of the interesting properties of horopter curves can be found in [9], [10], [7].

Up to our knowledge, horopter curves have not been used so far in their full potential for the self-calibration problem, with the remarkable exceptions of the works of Armstrong et al. [1] and of Schaffalitzky [15]. In the first one it is shown how horopters can be used for the recovery of the plane at infinity in the special case of planar camera motions. In the second the properties of horopter curves are employed to obtain new polynomial equations for the obtainment of the plane at infinity.

All the previously mentioned methods, as well as the present work, deal with the recovery of arbitrary but constant intrinsic parameters of the camera. Research has also been conducted elsewhere to cover the case of varying intrinsic parameters with some restrictions (see e.g., [8] and the references therein).

The main idea behind the algorithms is to take advantage of the highly singular configuration adopted by the horopter curves in relation with the plane at infinity and the absolute conic, which is preserved by homographies of the space. Then, starting from a projective calibration, this allows for the definition of cost functions on the set of planes of the space which vanish for the plane at infinity independently of the adopted projective coordinates. The minimization is carried out by means of a Levenberg-Marquardt algorithm.

Experiments show the good convergence and stability properties of the technique, even in the presence of noise, along with its computationally efficiency. Besides, the approach does not require the precise initialization which is usually imperative.

The paper is organized as follows: Section 2 reviews the projective camera model and formalizes the self-calibration problem. Section 3 provides a self-contained presentation of the relevant properties of horopter curves.

Some of these properties are new and for the others we have provided new proofs toward a more consistent and geometric-oriented presentation. Section 3 describes the algorithms and, finally, Section 4 provides the experimental results. The main contributions of this work, appart from the autocalibration algorithms, consist in relating horopter curves with the unimodular constraint of [12], which is done in Theorems 3.1.3 and 3.2. Theorems 3.5 and 3.6 also present new results concerning the geometry of horopter curves.

2. MATHEMATICAL MODEL OF CAMERA SELF-CALIBRATION

Our model for a real camera will be the traditional pinhole camera [3], which is defined by its optical center C and the image plane π. The image plane is endowed with an affine coordinate system $(O; \mathbf{u}, \mathbf{v})$, where $O \in \pi$ is an arbitrary origin of coordinates and vectors $\mathbf{u}$ and $\mathbf{v}$ form a basis of the plane, not necessarily orthonormal. In practice this coordinate system is that given by the pixel structure of the camera. The capture of the 3D-scene is then mathematically modeled as the correspondence of each space point with its projection onto the plane π with center C.

For convenience, we consider the Euclidean space coordinate system $\{C; \mathbf{x}, \mathbf{y}, \mathbf{z}\}$ where $\mathbf{x} = \mathbf{u}/\|\mathbf{u}\|$, $\mathbf{y}$ is defined so that $\{\mathbf{x}, \mathbf{y}\}$ is an orthonormal basis of π with the same orientation of $\{\mathbf{u}, \mathbf{v}\}$, and $\mathbf{z}$ completes them to an orthonormal basis and points toward the camera from C.

Using homogeneous coordinates attached to the previously defined references, say $Q^c = (x^c, y^c, z^c, t^c)^T$ and $q = (u, v, w)^T$ for space and image points, respectively, the equations of the projection are

$$q = \lambda K (I \,|\, \mathbf{0}) \, Q^c,$$

where I is the 3×3 identity matrix, λ is a projective proportionality constant, and K is the matrix of intrinsic parameters given by

$$K = \begin{pmatrix} -\dfrac{f}{\|\mathbf{u}\|} & \dfrac{f \cot \theta}{\|\mathbf{u}\|} & u_0 \\ 0 & -\dfrac{f}{\|\mathbf{v}\| \sin \theta} & v_0 \\ 0 & 0 & 1 \end{pmatrix}.$$

In this matrix f is the focal length, i.e., the Euclidean distance from the optical center to the image plane, θ is the angle from $\mathbf{u}$ to $\mathbf{v}$, and $(u_0, v_0)^T$ are the non-homogeneous image coordinates of the principal point, i.e., the orthogonal projection of C onto π [3].

More generally, if we want to use and arbitrary Euclidean space coordinate system instead of the one associated to the camera, the projection equations become

$$q = \lambda K \left(R \,|\, \mathbf{t} \right) Q^e$$

where $Q^e = (x, y, z, t)^T$ are the space point homogeneous coordinates in the new reference and R and $\mathbf{t}$ are respectively the rotation matrix and translation vector giving the motion from the second to the first space systems.

Even more generally, we can use an arbitrary projective 3D coordinate system instead of an Euclidean one, with coordinates $Q = (X, Y, Z, T)^T$ related to the Euclidean coordinates by a 4×4 regular matrix G so that

$$Q^e = \mu \, G \, Q,$$

where μ is a projective proportionality constant. In this case the equation of the projection is given by

$$q = \nu P Q$$

where $P = K \left(R \,|\, \mathbf{t} \right) G$ and we have abbreviated $\nu = \lambda \mu$.

The knowledge of the projection matrix P referred to the mentioned 3D projective coordinate system and the 2D affine coordinate system of the camera is called a *projective calibration* of the camera. In the case of multiple cameras, a projective calibration of the set is the knowledge of their projection matrices with respect to a common projective space reference and their respective image plane references. An important issue is to obtain a projective calibration respeting the convex hull of the points in the image (see [6], [11]).

The affine calibration of the set of cameras consist in the obtainment of the projection matrices with respect to any affine space reference. We recall that an affine reference is just a projective reference $\{\mathbf{X}_0, \mathbf{X}_1, \mathbf{X}_2, \mathbf{X}_3, \mathbf{E}\}$ such that $\mathbf{X}_1, \mathbf{X}_2$ and $\mathbf{X}_3$ belong to the plane at infinity (see [16]). Therefore the affine calibration can be achieved by determining the coordinates of the plane at infinity.

Analogously, an Euclidean calibration is an affine calibration for which the affine reference is Euclidean, i.e., such that the absolute conic has equations

$$X^2 + Y^2 + Z^2 = T = 0.$$

This corresponds to the usual notion that the basis of the associated Cartesian reference is orthonormal (up to a scale factor).

3. HOROPTER CURVES

3.1. **Definition and basic properties.** Let us consider two cameras identical in every respect but in their space position. This means that each element of the second camera can be obtained from the corresponding element of the first one by applying to it a common Euclidean motion. The set of 3D points whose projections on both cameras have identical coordinates is called the horopter associated to the pair of cameras. In this paper we will only develop those properties of the horopter curves which are related to the recovery of intrinsic and extrinsic parameters. The interested reader may consult [9], [10], [7] for related information on the subject.

Let us compute the equation of the horopter associated with a couple of cameras with projection matrices $P_i = \lambda_i K(R_i \,|\, \mathbf{t}_i)G$, $i = 1, 2$. A point Q projects onto each camera on points of the same homogeneous projective coordinates if and only if

$$(1) \qquad\qquad P_1 Q = \theta P_2 Q,$$

for some constant $\theta \in \mathbf{C} \cup \{\infty\} = \mathbf{P}^1$ understood as a projective parameter, in the sense of [16]. Note that the particular cases $\theta = 0$ or $\theta = \infty$ correspond to the camera centers, which always belong to the horopter. Equation (1) means that Q belongs to the null-space of the matrix $P_1 - \theta P_2$. To compute this kernel, let us denote by a_i^T, b_i^T and c_i^T the rows of the matrix P_i. A point Q is in this kernel if and only if it satisfies the system of equations

$$(a_1^T - \theta a_2^T)Q = 0$$
$$(b_1^T - \theta b_2^T)Q = 0$$
$$(c_1^T - \theta c_2^T)Q = 0.$$

This means that Q lies simultaneously in the planes of coordinates $a_1 - \theta a_2$, $b_1 - \theta b_2$ and $c_1 - \theta c_2$. Let us denote by $\alpha = (\alpha_1, \alpha_2, \alpha_3, \alpha_4)^T$ the coefficients of a generic plane. The planes of the star through Q (we recall –see [16]– that this is the set of planes and lines containing Q) are given by the equation

$$\det(\alpha, a_1 - \theta a_2, b_1 - \theta b_2, c_1 - \theta c_2) = 0.$$

The coordinates of Q are therefore the coefficients of $(\alpha_1, \alpha_2, \alpha_3, \alpha_4)$ in this equation. From this we see that the homogeneous coordinates of Q are given by four polynomials of degree three in θ. Generically, these polynomials are independent and the horopter is therefore a twisted cubic. For more information on twisted cubics, see [16]. We will denote the parametric equation of the horopter by $h = h(\theta)$.

3.2. **The horopter and the absolute conic.** Being the horopter a cubic curve, it generically meets each plane in three points (maybe of complex coordinates). Let us denote the plane at infinity by π_∞. A point $Q \in \pi_\infty$ of Euclidean coordinates $Q^e \sim G^{-1}Q = (x, y, z, 0)^T$ belongs to the horopter if and only if

$$(P_1 - \theta P_2)Q \sim K(\lambda_1 R_1 - \theta \lambda_2 R_2 | \lambda_1 \mathbf{t_1} - \theta \lambda_2 \mathbf{t_2})Q^e = 0.$$

Setting $\hat{Q}^e = (x, y, z)^T$ and $\alpha = \lambda_2/\lambda_1$, this is equivalent to

$$(R_1 - \alpha \theta R_2)\hat{Q}^e = 0 \iff (R_2^T R_1 - \alpha \theta I)\hat{Q}^e = 0.$$

Observe that $R = R_2^T R_1$ is the rotation part of the motion carrying the first camera to the second one. The last equation means that $\hat{Q}^e$ is an eigenvector of R with eigenvalue $\alpha\theta$. Being R a rotation matrix, its eigenvalues are 1, $e^{i\varphi}$ and $e^{-i\varphi}$ where φ is the rotation angle. The eigenvector associated with the eigenvalue $\alpha\theta = 1$ must be real and corresponds to the direction of the rotation axis. Considering an eigenvector $\hat{Q}^e$ of eigenvalue $e^{i\varphi}$ we have that

$$\hat{Q}^{eT}\hat{Q}^e = \hat{Q}^{eT}R^T R\hat{Q}^e = (R\hat{Q}^e)^T(R\hat{Q}^e) = e^{i\varphi}\hat{Q}^{eT}e^{i\varphi}\hat{Q}^e = e^{2i\varphi}\hat{Q}^{eT}\hat{Q}^e.$$

So, as long as $e^{2i\varphi} \neq 1$, i.e, $\varphi \neq 0, \pi$ (as we will assume from now on) we obtain that $\hat{Q}^{eT}\hat{Q}^e = 0$, i.e, its coordinates satisfy the equation

$$x^2 + y^2 + z^2 = 0.$$

This means that the complex eigenvectors are points of the absolute conic (see [16], [3] for information on the absolute conic and how it encodes the Euclidean –or, more precisely, conformal– structure of the space).

Denoting by $\hat{Q}_0^e$ the real eigenvector and by $\hat{Q}_1^e$, $\hat{Q}_2^e$ the complex conjugate eigenvectors of R, a similar computation shows that

$$\hat{Q}_0^{eT}\hat{Q}_1^e = \hat{Q}_0^{eT}\hat{Q}_2^e = 0,$$

provided that $\varphi \neq 0$. This means that the polar line of the point of coordinates $\hat{Q}_0^e$ with respect to the absolute conic is the line through the points of coordinates $\hat{Q}_1^e$ and $\hat{Q}_2^e$. So we have the following result:

Theorem 3.1.   (1) *The horopter curve attached to a pair of cameras related with a motion of angle different from 0 and π intersects the plane at infinity at three points, one of which is real and the other two are complex conjugate and lie on the absolute conic.*
   (2) *The pole of the line determined by the complex points is the real one and the real point represents the direction of the screw axis of the motion.*[1]
   (3) *The horopter reaches the plane at infinity at parameters with ratios*
$$1 : e^{i\varphi} : e^{-i\varphi},$$
   φ being the rotation angle of the motion. In particular, the three parameters have the same modulus.

Remark 3.1. Since all the cameras share the same calibration matrix, the retinal coordinates provide us with natural isomorphisms among them, relating points with the same coordinates in different retinal planes. Therefore we can identify these planes with a virtual retinal plane Π endowed with coordinates (u, v, w) compatible with the isomorphisms and project onto it the intersection points and the absolute conic using any of the projection matrices (or even all of them). A relevant feature of this construction is that, as is well known (see [7]), the absolute conic projects onto the same conic of Π independently of the projection matrix used.

The polarity relations are preserved by the homographies induced by these projections. Let us consider a set of n projectively calibrated cameras P_l, $l = 1, \ldots, n$ with identical intrinsic parameters. For each pair of cameras (i, j), $i < j$, we denote by $h^{ij} = h^{ij}(\theta)$ the corresponding horopter, by Q_k^{ij}, $k = 0, 1, 2$ its intersection points with π_∞ and by r_{kl}^{ij} the projection $r_{kl}^{ij} = P_l Q_k^{ij}$. Of course, $r_{ki}^{ij} = P_i Q_k^{ij} = P_j Q_k^{ij} = r_{kj}^{ij}$, but the other projections will be different, in general (see figure 1). If A is the definite symmetric matrix of the projected absolute conic in Π we have

$$(2) \qquad \left(r_{0l}^{ij}\right)^T A\, r_{kl}^{ij} = 0 \text{ and } \left(r_{kl}^{ij}\right)^T A\, r_{kl}^{ij} = 0,$$

where $k = 1, 2$, $1 \leq i < j \leq n$, and $l = 1, \ldots, n$.

Note that although the projected points r_{kl}^{ij}, $l \neq i, j$, are homographically related to the $r_{ki}^{ij} = r_{kj}^{ij}$, the consideration of all these points is not redundant in the context of the search for the plane at infinity. Indeed, if the candidate plane is the plane at infinity, this homography leaves invariant the projected absolute conic, but if this is not the case, invariance of the conic does not hold true, and therefore these additional constraints are not redundant.

These equations provide us with a method to recover the projection of the absolute conic from the knowledge of the coordinates of the plane at infinity. They are in the heart of our algorithms, as will be explained later.
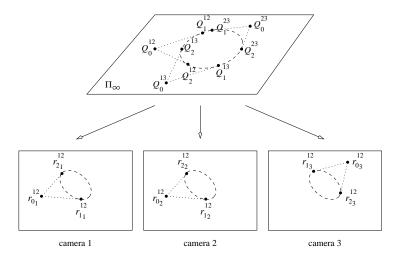

FIGURE 1. Diagram of relationships between the intersections of the horopters with the plane at infinity, the absolute conic, and their projections.

---

[1]This is just a projective version of the fact that the real line determined by the complex points is the direction of the pencil of planes orthogonal to the screw axis.

3.3. **Horopters and the unimodular constraint.** Twisted cubics can be generated by means of a homography relating two stars in space. For the convenience of the reader, we recall here this Steiner-type construction (see [16]).

The star of a point has a structure of projective plane and so we can consider homographies between stars. Such homographies can be generated using a homography of the ambient space $H : \mathbf{P}^3 \to \mathbf{P}^3$ as follows: For each pair of points C_1 and $C_2 = H(C_1)$ we can define a homography $\mathrm{Star}(C_1) \to \mathrm{Star}(C_2)$ just by sending the line $l \in \mathrm{Star}(C_1)$ (resp. the plane π) to the line $H(l) \in \mathrm{Star}(C_2)$ (resp. the plane $H(\pi)$). For simplicity, we will denote the homography between these stars again by H. Note that any homography between stars is induced by a homography of the ambient space: to see this it is enough to realize that a homography between stars is equivalent to a homography between two planes of the dual space $\mathbf{P}^{3\star}$, which has an infinity of extensions to the whole space.

In general, a line of the first star does not intersect its image. However, the set of lines which do intersect its image produce a twisted cubic, i.e., given a homography $H : \mathrm{Star}(C_1) \to \mathrm{Star}(C_2)$ the set

$$\{P \in \mathbf{P}^3 : P = l \cap H(l), l \in \mathrm{Star}(C_1)\}.$$

is a twisted cubic. And, conversely, every twisted cubic can be generated in this way.

The motion between the cameras is a homography of the space which induces the corresponding homography between the stars based on the optical centers of the cameras. The associated twisted cubic is the horopter previously defined. From this, it follows immediately that the horopter depends only on the relative motion between the cameras and the position of the first optical center.

So let us consider a homography $H : \mathrm{Star}(C_1) \to \mathrm{Star}(C_2)$. For each plane τ not containing neither of the points C_1 and C_2, there is a natural homography $H_\tau : \tau \to \tau$ induced by H, defined as follows: Given a point $Q \in \tau$, we define $H_\tau(Q) = H(C_1Q) \cap \tau$. Generically, a homography of a projective plane has three fixed points. By its very definition, the three fixed points of H_τ are the three intersection points of τ with the twisted cubic associated to H.

Theorem 3.2. (Unimodular constraint) *Let $H : \mathrm{Star}(C_1) \to \mathrm{Star}(C_2)$ be a homography and τ a plane not containing any of the centers of the stars. Let us consider the associated homography $H_\tau : \tau \to \tau$, which we suppose to be generic, in the sense that it has exactly three different fixed points, say, Q_0, Q_1 and Q_2. Let $h = h(\theta)$ be the twisted cubic attached to H, and let us denote by θ_i the parameters of the points Q_i for $i = 0, 1, 2$, and by μ_j the parameters of C_j, $j = 1, 2$. Then the eigenvalues λ_0, λ_1 and λ_2 of H_τ have ratios given by*

$$\frac{\lambda_0}{\lambda_2} = \{\mu_1, \mu_2, \theta_0, \theta_2\}, \quad \frac{\lambda_1}{\lambda_2} = \{\mu_1, \mu_2, \theta_1, \theta_2\}.$$

In the particular case that the centers are reached at parameters 0 and ∞, we have

$$\frac{\lambda_0}{\lambda_2} = \{0, \infty, \theta_0, \theta_2\} = \frac{\theta_0}{\theta_2}, \quad \frac{\lambda_1}{\lambda_2} = \{0, \infty, \theta_1, \theta_2\} = \frac{\theta_1}{\theta_2}.$$

Proof. Let us consider the projective reference $\{\mathbf{X}_0, \mathbf{X}_1, \mathbf{X}_2, \mathbf{X}_3, \mathbf{E}\}$ of $\mathbf{P}^3$, where $\mathbf{X}_0 = C_1, \mathbf{X}_1 = Q_0, \mathbf{X}_2 = Q_1, \mathbf{X}_3 = Q_2, \mathbf{E} = C_2$. In terms of this reference, the plane $\tau = X_1X_2X_3$ has equation $X = 0$. The cubic that reaches the points at the required parameters has the form

$$h(\theta) = \left(\frac{\mu_2 - \mu_1}{\theta - \mu_1}, \frac{\mu_2 - \theta_0}{\theta - \theta_0}, \frac{\mu_2 - \theta_1}{\theta - \theta_1}, \frac{\mu_2 - \theta_2}{\theta - \theta_2} \right).$$

as can be easily checked. To determine the homography H_τ we need to know the image of a fourth point. Note that the twisted cubic can be reparametrized by means of a homographic change of coordinate

$$\theta = \frac{a\theta' + b}{c\theta' + d}, \ ad - bc \neq 0$$

without affecting the cross ratios of the parameters. So we can assume, reparametrizing the curve if necessary, that none of the parameters λ_i, μ_j coincides with ∞. Then we can consider the point $Q = h(\infty) = (\mu_2 - \mu_1, \mu_2 - \theta_0, \mu_2 - \theta_1, \mu_2 - \theta_2)$. Since $H_\tau(C_1Q \cap \tau) = C_2Q \cap \tau$, the point $C_1Q \cap \tau = (0, \mu_2 - \theta_0, \mu_2 - \theta_1, \mu_2 - \theta_2)$ maps to the point of coordinates $(0, \mu_1 - \theta_0, \mu_1 - \theta_1, \mu_1 - \theta_2)$. Using now (Y, Z, T) as coordinates for the plane τ, the homography H_τ maps

$$(1, 0, 0) \mapsto (1, 0, 0)$$
$$(0, 1, 0) \mapsto (0, 1, 0)$$
$$(0, 0, 1) \mapsto (0, 0, 1)$$
$$(\mu_2 - \theta_0, \mu_2 - \theta_1, \mu_2 - \theta_2) \mapsto (\mu_1 - \theta_0, \mu_1 - \theta_1, \mu_1 - \theta_2)$$

and so it is given by a matrix of the form (up to multiples)

$$H_\tau \equiv \begin{pmatrix} \frac{\mu_1-\theta_0}{\mu_2-\theta_0} & 0 & 0 \\ 0 & \frac{\mu_1-\theta_1}{\mu_2-\theta_1} & 0 \\ 0 & 0 & \frac{\mu_1-\theta_2}{\mu_2-\theta_2} \end{pmatrix},$$

so $\lambda_0 : \lambda_1 : \lambda_2 = \frac{\mu_1-\theta_0}{\mu_2-\theta_0} : \frac{\mu_1-\theta_1}{\mu_2-\theta_1} : \frac{\mu_1-\theta_2}{\mu_2-\theta_2}$ from which the result follows.   □

Since we have seen that in the particular case of an horopter attached to a pair of cameras with identical intrinsic parameters the optical centers are reached by the horopter at $\theta = 0, \infty$, we obtain that the eigenvalues λ_0, λ_1 and λ_2 of the inter-image homography induced by the plane at infinity are in the same ratio that the parameters θ_0, θ_1 and θ_2 at which the horopter reaches the plane at infinity, i.e.,

$$\lambda_0 : \lambda_1 : \lambda_2 = \theta_0 : \theta_1 : \theta_2.$$

This equality, together with Theorem 3.1.3 implies the unimodular constraint introduced by Pollefeys et al. [12]. Compare with [15].

Next Theorem shows how the parameters of these points are related with the eigenvalues of H_τ. Note that this result, together with Theorem 3.1.3 implies the unimodular constraint

3.4. **Cones and horopters.** There is a 2-parameter family of quadrics containing a given twisted cubic (see [16]), and this relates the horopter with the ambiguity phenomenon (see the interesting book of Maybank [10] for more information on this subject).

For each point P of the twisted cubic, the set of rays joining P with all the other points of the cubic is a cone, including the tangent line at P as a limit case. To see this, it is enough to check that the curve obtained intersecting this surface with a plane not including P is a conic. According to Bezout's Theorem it is enough to see that a generic line on the plane intersects the curve in just two points. To find them is equivalent to finding the intersections, different from P, of the plane determined by the line and P with the twisted cubic. These intersection are, in general, three points, the vertex P and two other ones. This means that the curve is a conic and therefore that the ruled surface is a cone (cf. [16]).

In the particular case of an horopter curve, we can consider the cone with vertex the real point at infinity of the horopter, Q_0, which is a cylinder. To see what type of conic is the base of this cylinder, let us consider a plane orthogonal to the axis of the cylinder, i.e., a plane intersecting the plane at infinity in the polar line of Q_0 with respect the absolute conic. By Theorem 3.1, this plane contains the complex conjugate points of the horopter at infinity, Q_1 and Q_2, the cyclic points at infinity of the plane. Therefore the conic is a circle (see figure 2). We have proved the following Theorem (this result is well known and frequently mentioned in the literature, e.g., [14]).

Theorem 3.3. *The horopter curve is contained within a circular cylinder formed by all the lines touching the horopter with the same direction that the screw axis of the motion.*
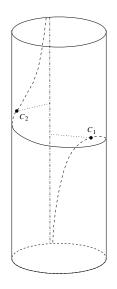

FIGURE 2. An horopter in its cylinder showing the screw axis of the motion.

For the sake of completeness, we include the following property. Let us construct a cone containing the horopter taking as vertex one of the optical centers. The curve obtained intersecting the cone with the corresponding retinal plane is a conic. It is not difficult to find the equation of this conic: If the points q and q' are the images in the first and second cameras, respectively, of the same point in space, then their coordinates satisfy the relation $q^T F q' = 0$, where F is the fundamental matrix of the pair. If q and q' are the images of a point of the horopter $h(\theta)$, then q and q' have the same coordinates. We abuse notation and write $q = q'$. Therefore $q^T F q = 0$ If we decompose $F = F_S + F_A$ as a sum of its symmetric part $F_S = (F + F^T)/2$ and its antisymmetric part $F_A = (F - F^T)/2$, we have that $q^T F q = q^T F_S q = 0$, i.e., q lies over a conic of matrix F_S. Note that although F is a singular matrix, its antisymmetric part is not singular, in general. So we have proved the following Theorem, which can also be found in [7]).

Theorem 3.4. *The projection of the horopter on each retina of the camera pair is a conic with matrix the symmetric part of the fundamental matrix of the pair.*

3.5. **Other properties of the horopters.** Given a plane $\pi \in \mathrm{Star}(C_1)$ let us consider its image $\pi' = H(\pi) \in \mathrm{Star}(C_2)$, which we suppose to be different from π. Let us consider the line $l = \pi \cap \pi'$, which we suppose different from $C_1 C_2$. Then H induces a homography on l, sending each $P \in l$ to the point $P' = H(C_1 P) \cap l$. Any homography of a line has either two different fixed points, or one double fixed point. Note that the fixed points belong to the associated twisted cubic, so l is a chord of this cubic. If we have a double fixed point on l then l is tangent to the twisted cubic at that point.

In the particular case of the horopter curve, let l be the screw axis of the motion and π the plane determined by C_1 and l. Being the screw axis invariant under the motion, the image of π is the plane π' determined by C_2 and l. Hence the screw axis $l = \pi \cap \pi'$ is a chord of the horopter. But, since the motion acts on l as a translation (assuming that the motion is not a pure rotation), the only fixed point of the homography induced on l is the point at infinity, which is double. So we have the following Theorem:

Theorem 3.5. *If the motion between the cameras is not a pure traslation, then the tangent to the horopter at its real point at infinity is the screw axis of the motion.*

Proof. We have already considered the case of a generic motion. If the motion is a pure rotation, the horopter factorices in a line (the screw axis) and a circle, and so the Theorem holds true. □

Let us now study the effect of a coordinate change on the horopter curve. So we have new projective coordinates $\bar{Q} = (\bar{X}, \bar{Y}, \bar{Z}, \bar{T})^T$ related with the former ones by a non-singular matrix A as follows: $\bar{Q} = G Q$. Then we will have new camera matrices $\bar{P}_i = \nu_i P_i G^{-1}$, and the horopter $\bar{h} = \bar{h}(\bar{\theta})$ is defined by

$$0 = (\bar{P}_1 - \bar{\theta} \bar{P}_2) \bar{h}(\bar{\theta}) = (\nu_1 P_1 - \nu_2 \bar{\theta} P_2) G^{-1} \bar{h}(\bar{\theta}),$$

therefore

$$\bar{h}(\bar{\theta}) = G\, h \left(\frac{\nu_2}{\nu_1} \bar{\theta} \right).$$

We see from this that for a given coordinate system and an order of the cameras all the possible parameterizations of the corresponding horopter are related by a coordinate change of the form $\theta = k \bar{\theta}$, $k \neq 0$. In any of these parameterizations the optical center of the first camera is reached at $\theta = 0$ and that of the second camera is reached at $\theta = \infty$. If there is no privileged order of cameras, we must also consider changes of parameter of the form $\theta = k/\bar{\theta}$, as it follows from equation [1]. So we have the following Theorem:

Theorem 3.6. *Under a change of projective coordinates $\bar{Q} = G\, Q$, the corresponding horopter $\bar{h} = \bar{h}(\bar{\theta})$ is related to $h = h(\theta)$ by*

$$\bar{h}(\bar{\theta}) = G h \left(\lambda \bar{\theta} \right) \text{ or } \bar{h}(\bar{\theta}) = G h \left(\frac{\lambda}{\bar{\theta}} \right)$$

according to whether we interchange or not the order of the cameras and where λ is a constant which depends on the choice of the representatives of the matrices of the cameras. The parameters 0 and ∞ always correspond to the optical centers of the cameras.

4. Camera self-calibration using horopter curves

In this section we propose two different algorithms based on the properties of the horopters introduced above. The first algorithm consists in a stratified calibration which first provides the plane at infinity and then the absolute conic. Its first phase (affine calibration) can be seen as an implementation of the unimodular constraint algorithm of [12] in terms of horopter curves. The second phase (Euclidean calibration) provides the absolute conic by

estimating linearly the best-fit conic with respect to the intersections of the horopters with the plane at infinity (relations given in Theorem 3.1).

The second one gives directly the Euclidean structure of space. While the first algorithm is computationally simpler, the second one is more robust in the presence of noise, as we will see in the next section. Both algorithms use general purpose optimization techniques (a Levenberg-Marquardt algorithm as in [13]).

4.1. **Algorithm 1: Horopters and the unimodular constraint.** This algorithm operates in two phases. In the first one the plane at infinity is obtained by means of an optimization process in which the target function is based on the unimodular constraint. The second phase provides the projected absolute conic in a direct fashion using the relationships given in Remark 3.1.

The cost function employed for the affine calibration assigns to a candidate plane of coordinates $u = (u_0, u_1, u_2, u_3)$ the quantity

$$c_1(u) = \sum_{\substack{i,j=1 \\ i<j}}^{n} \sum_{\substack{k,l=1 \\ k \neq l}}^{2} \left(\left| \frac{\theta_k^{ij}}{\theta_l^{ij}} \right| - 1 \right)^2,$$

where $\theta_0^{ij}, \theta_1^{ij}, \theta_2^{ij}$ are the parameters of the points of intersection of the plane u with the horopter associated to the camera pair (i,j). This cost function has been designed to be invariant under permutations and scaling of the parameters. Note that with an adequate parameterization of the space of planes, this leads to a three-dimensional search. In practice, this will be achieved by selecting one of the u_i to be one. It would also be possible to carry out just a two-dimensional search using as parameters the modulus and the phase of the θ_k^{ij} for a given horopter h^{ij}. However, numerical instability has been observed, which discourages this approach. Besides, three-dimensional search turns out to perform quite efficiently, as will be explained in the following section.

Note that the computational cost of one evaluation of c_1 is essentially that of finding the roots of a third degree polynomial equation. For the starting point of the optimization process, a first guess of the plane at infinity is obtained by means of a linear algorithm which provides an exact solution if the cameras are orthogonal, i.e., if K is a diagonal matrix (see [17]). The good convergence properties of the algorithm allow to employ a starting point obtained by this method even if the camera is very far from verifying this condition, as will be seen in the section of results.

Once the plane at infinity has been found, different linear methods can be employed to calculate the projection of the absolute conic (see e.g. [12]). The properties of the horopters provide new linear methods for this task. A first approach would be to estimate the absolute conic as the best-fit conic in the plane at infinity with respect to the incidence and polarity relations given by Theorem 3.1. This would require the definition of a suitable projective reference in this plane. To avoid this, we take advantage of the constrution in Remark 3.1 by projecting the intersection points onto the virtual plane Π and calculating the best-fit conic with respect to equations (2). The obtained conic is the projection of the absolute conic, whose matrix is given by $A = (KK^T)^{-1}$, so that the intrinsic parameter matrix can be obtained from it by means of Cholesky factorization.

4.2. **Algorithm 2: Horopters and absolute conic.** This algorithm is an alternative to the previous one in which both affine and Euclidean calibration are performed at the same time by means of an optimization process. The new target function measures to what extent a candidate plane verifies equations (2). For the sake of clarity we define this function in two steps. First, we associate to a given plane of coordinates $u = (u_0, u_1, u_2, u_3)^T$ and a symmetric matrix A the number $f(u, A)$ given by

$$f(u, A) = \sum_{i<j}^{n} \sum_{l} \left\{ \left| \left(r_{0l}^{ij} \right)^T A\, r_{kl}^{ij} \right|^2 + \sum_{k=1}^{2} \left| \left(r_{kl}^{ij} \right)^T A\, r_{kl}^{ij} \right|^2 \right\}$$

with notations as in Remark 3.1 and taking normalized representatives of the r_{kl}^{ij}. This is a quadratic form in the coefficients of A, so with respect to these coefficients standard minimization can be applied: We write

$$f(u, A) = a^T M a$$

where M is a 6×6 matrix whose entries depend on the r_{kl}^{ij} and $a^T = (a_1, \ldots, a_6)$ where

$$A = \begin{pmatrix} a_1 & a_2 & a_3 \\ a_2 & a_4 & a_5 \\ a_3 & a_5 & a_6 \end{pmatrix}.$$

Then we define the cost of the plane u as

$$c(u) = \min_{\|a\|=1} f(u, A)$$

where $\|a\|$ stands for the Euclidean norm of the vector.

Then $c(u)$ is given by the minimum eigenvalue of M and the vector a is the corresponding eigenvector. If u is the true plane at infinity, this eigenvalue must be zero, since the best-fit conic meets exactly all the constraints. Although there are more sophisticated methods to find the best-fit conic, we will see in the following section that this linear technique suffices to provide satisfactory results.

The risk that the optimization process leads to a spurious minimum motivates the introduction of additional terms in the cost function. As the matrix of the projected absolute conic is definite, penalty terms have been included in the target function to increase the cost of a candidate plane leading to a non-definite matrix. The finally selected target function has the form

$$c_2(u) = c(u)g_1(A_u) + \alpha g_2(A_u)$$

where A_u is the normalized symmetric matrix that minimizes $f(u, A)$ for the plane u, $g_1(A)$ is the penalty for closeness to singularity, $g_2(A)$ is that for non-definiteness and α is a weighting factor. We define

$$g_1(A) = 1 + 1/|\lambda_{\min}|^p$$

$$g_2(A) = \sum_{\mathrm{sign}(\lambda_i) \neq \mathrm{sign}(\lambda_{\max})} |\lambda_i|$$

where $\lambda_{\min}$ (resp. $\lambda_{\max}$) is the eigenvalue of A of minimum (resp. maximum) absolute value, p is a suitable power and (λ_i) is the sequence of eigenvalues of A. In our experiments we have taken $\alpha = 10^{12}$, $p = 6$.

The initialization of the algorithm is the same as that of the previous one, and it is also robust with respect to the starting point. However, as we next see, it is more robust with respect to noise.

5. Experimental results

To evaluate the performance of the techniques a scenario has been simulated in which a set of three cameras capture a scene consisting in a set of 100 randomly positioned 3D points. The Euclidean coordinates of these points are obtained from a uniform distribution with support a centered cube of side two units. The three cameras are located at random with principal axes passing close to the center of the point distribution.

More specifically, the first camera has optical center $C_1 = -\mathbf{t}_1 = (0, 0, d)^T$ and projects onto plane $z = h$, so that its projection matrix in standard form can be written as $P_1 = K(I \,|\, \mathbf{t}_1)$. The other cameras are randomly rotated and translated versions of the first one, with projection matrices $P_i = K(R_i \,|\, \mathbf{t}_i)$, where the R_i are random rotation matrices ranging over the whole rotation group, and $\mathbf{t}_i = R_i \mathbf{t}_1 + \Delta \mathbf{t}_i$, with the $\Delta \mathbf{t}_i$ random vectors with independent components uniformly distributed within $[-s, s]$. This arrangement intends to model a set of cameras approximately pointing toward the center of coordinates, and located all of them at a similar distance of this center. We project the 3D points and perturb the resulting affine coordinates with noise of independent components uniformly distributed within $[-n, n]$.

The values of the intrinsic parameters have been taken so that the projections lie roughly within the range that would be typical for values measured in pixels of images obtained with a video camera.

Projective calibration is first performed by camera pairs using the algorithm described in [5]. The estimation of the fundamental matrix is computed by means of the elementary eight-point algorithm [7]. Then five of the observed 3D points are selected at random to establish a common projective basis.

We parameterize the space of planes just by setting one of the components of the plane coordinates $u = (u_0, u_1, u_2, u_3)^T$ to be one. In practice, a very slight improvement is observed if the four possible choices are employed and the result of minimum cost is selected, which is what we do in our experiments.

Although the geometry of the algorithms is independent of scaling, its numerical procedures are not: For example, the extraction of eigenvalues is scaling-dependent. In practice, scaling of the data has proved to be very significant in the performance of the algorithms. In our case, a homothety $(u, v) \mapsto (\lambda u, \lambda v)$ is applied to the non-homogeneous affine observed noisy coordinates, and its effects are corrected in the output of the algorithm. A rule of thumb for the value of λ is to take it as the inverse of the maximum observed coordinate.

For a given selection of intrinsic parameters and noise level, a set of 300 different experiments is considered, each with a different set of camera positions and 3D point coordinates. With high noise levels the algorithms fail occasionally to provide a definite matrix for the estimated absolute conic. This limitation is easily overcome by reprocessing the data with a different choice for the projective basis. As each optimization takes a few seconds for the second algorithm (on a Intel Pentium 4 machine running under Linux at 1500 MHz), which is the most costly, this redundancy is perfectly affordable. In our experiments each processing is actually performed with different basis until three different successes are obtained (with a maximum of ten attempts), and the minimum cost solution is selected.

Figure 3 show the average relative error curves for the first (figure 3.a) and second (figure 3.b) algorithms together with the corresponding curves and for two intermediate algorithms resulting from two different combinations of the cost functions $\beta_1 c_1 + \beta_2 c_2$ (figure 3.c and 3.d). We consider the case of three cameras with parameters indicated in the caption. Figure 4 shows analogous results for a different set of intrinsic parameters.

These results clearly show that the increase in computational cost of algorithm 2 is justified by an improvement in performance. Besides, it is seen that a combination of both cost functions does not necessarily imply an additional gain.

Nacho: tienes que meter ms figuras

References

[1] M. Armstrong, A. Zisserman, R. Hartley, Self-calibration from image triplets, , In *European Conference of Computer Vision*, pages 3–16. 1996

[2] S. Maybank and O. Faugeras, A theory of self–calibration of a moving camera. In *International Journal of Computer Vision*, 8 (2), pages 123–141. 1992

[3] O. Faugeras, *Three-Dimensional Computer Vision: A Geometric Viewpoint*, MIT Press, Cambridge, Massachusetts. 1993

[4] A. Fusiello, Uncalibrated Euclidean reconstruction: a review. In *Image and Video Computing*, 18, pages 555-563, 2000.

[5] R.I. Hartley, Projective reconstruction and invariants from multiple images, In *IEEE Trans. on PAMI*, vol. 16, no. 10, Oct. 1994.

[6] R. I. Hartley, Chirality, *International Journal of Computer Vision*, 26 (1), pp. 41-46, 1998.

[7] R.I. Hartley and A. Zisserman, *Multiple View Geometry in Computer Vision*. Cambridge University Press, Cambridge, UK, 2000.

[8] R.I. Hartley, E. Haymann, L. de Agapito and I. Reid, Camera calibration and the search for infinity. In *Proceedings of the International Conference on Computer Vision*, 1999.

[9] S.J. Maybank, The Projective Geometry of Ambiguous Surfaces. In *Philosophical Transactions: Physical Sciences and Engineering*, 332 (1623), pages 1–47, 1990.

[10] S.J. Maybank, *Reconstruction from projections*, Springer-Verlag, Berlin, 1993.

[11] D. Nister, Calibration with robust use of cheirality by quasi-affine reconstruction of the set of camera projection centres, In *Proceedings 8th IEEE International Conference on Computer Vision. ICCV 2001*, 2001, pp. 116-23, vol.2.

[12] M. Pollefeys, L. Van Gool, Stratified self-calibration with the modulus constraint, In *IEEE Trans. on Pattern Analysis and Machine Intelligence*, 21 (6), pages 707-724. 1999.

[13] W.H. Press et al., *Numerical Recipes in C++: The Art of Scientific Computing, 2nd. ed.*. Cambridge University Press, Cambridge, MA. 2002.

[14] L. Quan and Z. Lan, Linear N-Point Camera Pose Determination. In *IEEE Transactions on Pattern Analysis and Machine Intelligence*, vol. 21, no. 8, pages 774–780, 1999.

[15] F. Schaffalitzky, Direct Solution of Modulus Constraints. In *Proc. Indian Conference on Computer Vision, Graphics and Image Processing, Bangalore*. 2000.

[16] J.G. Semple and G.T. Kneebone, *Algebraic Projective Geometry*, Oxford Classic Texts in Physical Sciences, Oxford University Press, Oxford, 1998.

[17] Y. Seo, A. Heyden, Auto-calibration from the orthogonality constraints, In *International Conference on Computer Vision*, Barcelona, Spain, 2000.

[18] W. Triggs, Auto-calibration and the absolute quadric. In *Proc. IEEE Conference on Computer Vision and Pattern Recognition*, pages 609–614. 1997.
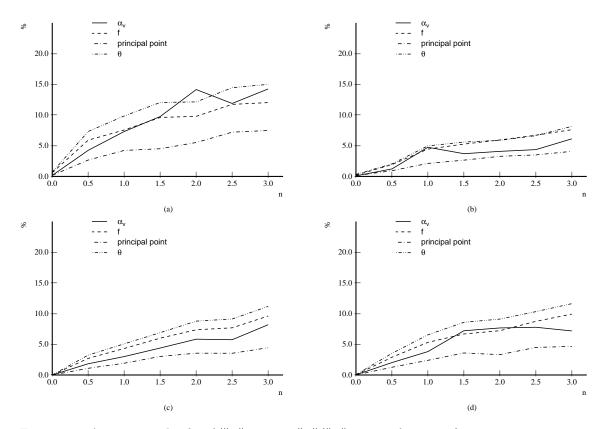
FIGURE 3. Average results for $f/\|\mathbf{u}\| = 250$, $\|\mathbf{v}\|/\|\mathbf{u}\| = 1.5$, $\theta = 0.8\pi/2$, $u_0 = 80$, $v_0 = 80$, $d = 1.6$, $s = 0.1$, and noise amplitud n from 0 to 3 pixels. In (c) $\beta_1 = 1$, $\beta_2 = 10^2$. In (d) $\beta_1 = 1$, $\beta_2 = 10^5$.
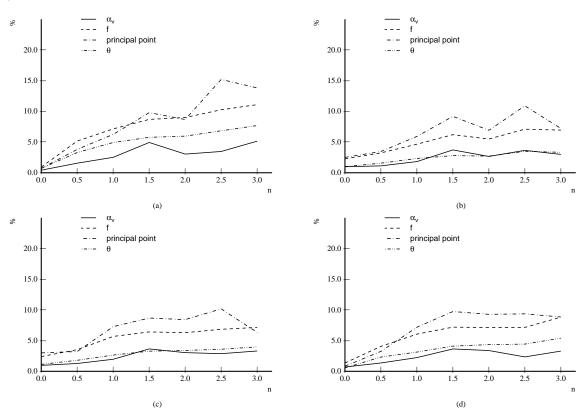

FIGURE 4. Average results for $f/\|\mathbf{u}\| = 1000$, $\|\mathbf{v}\|/\|\mathbf{u}\| = 1$, $\theta = \pi/2$, $u_0 = 250$, $v_0 = 250$, other parameters as in previous figure.